CHAPTER EIGHT: OCCURRENCE, DESCRIPTION AND CHEMICAL COMPOSITION OF THE OPAQUE MINERALS

In this chapter, the base metal sulphides, their occurrence and composition as well as the possible evolution of the sulphide assemblages at Nonnenwerth and Townlands will be described and discussed.

8.1 Sulphide and oxide minerals on Nonnenwerth

8.1.1 Platreef gabbronorite

The gabbronorite is generally barren or weakly mineralized and typically contains less than 1 vol. % sulphides (locally up to 4 vol. %) and up to 5 vol. % magnetite, chromite and ilmenite. The sulphides consist of pyrrhotite (50 – 70 %), chalcopyrite (10 – 40 %), pentlandite (5 – 10 %) and traces of pyrite, sphalerite and mackinawite. The sulphides occur as mm-sized, composite grains interstitial to or included in silicates, and as µm-sized disseminations in altered silicate minerals mostly forming aureoles around massive composite sulphides.

Pyrrhotite forms micron- to millimetre-sized grains that are often intergrown with chalcopyrite and pentlandite and may carry flame-like exsolution lamellae of the latter (Fig. 8.1a, b and c). The mineral rarely forms monomineralic grains. Chalcopyrite and pentlandite mostly occur along the margins of pyrrhotite grains (Figs 8.1c, d and e), or along fractures within pyrrhotite. Chalcopyrite also occurs as disseminations in aureoles around composite pyrrhotite, chalcopyrite and

pentlandite grains (Fig. 8.1b, d and e). The disseminated chalcopyrite is intergrown with secondary hydrosilicates adjacent to composite sulphide grains. Chalcopyrite often contains fine flame-like exsolutions of mackinawite and may include up to 10 µm wide disseminated sphalerite grains. In places, anhedral, micron-sized chalcopyrite occurs included in magnetite and may be intergrown with pentlandite (Fig. 8.1f).

Pentlandite occurs as polycrystalline fragmented grains along fractures in pyrrhotite or towards pyrrhotite grain margins (Fig. 8.1c and d), and as flame-like exsolution lamellae oriented along a single crystallographic axis (Fig. 8.1b). Only one grain of anhedral or subhedral pyrite enclosed in plagioclase was identified. Magnetite is anhedral or subhedral, commonly fractured (Fig. 8.1f) and occurs interstitial to silicates. It is often intergrown with ilmenite and in places encloses anhedral chalcopyrite and pentlandite grains (Fig. 8.1f). Ilmenite is internally homogenous. It is mostly intergrown with composite grains of pyrrhotite with minor pentlandite and chalcopyrite (Fig. 8.1d and e).

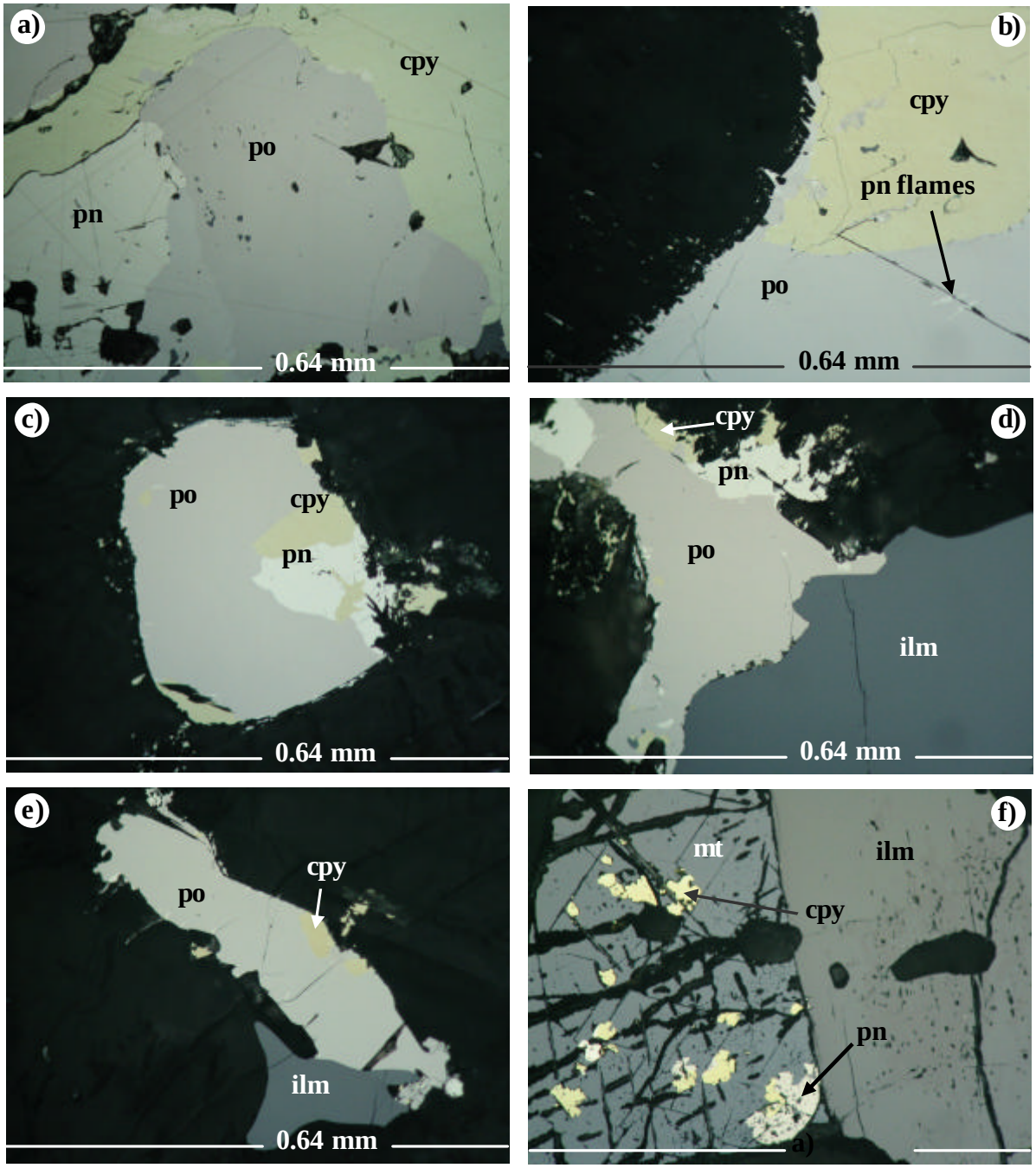

Fig. 8.1: Photomicrographs:
(a) Pyrrhotite (po) intergrown with pentlandite (pn) and chalcopyrite (cpy) (sample MOX11). b) Pyrrhotite and chalcopyrite intergrowth. Dark material is silicate. Note the pentlandite flames in pyrrhotite and the fine pyrrhotite injections into adjacent silicate (sample MOX15). (c) Pyrrhotite intergrown with minor pentlandite and chalcopyrite (sample MOX15). (d & e) Anhedral pyrrhotite intergrown with ilmenite (ilm). Minor chalcopyrite and pentlandite occur along the grain margin of pyrrhotite. Note the fine disseminations of chalcopyrite in adjacent silicates (sample MOX15). (f) Fractured magnetite (mt) intergrown with ilmenite. Magnetite encloses anhedral chalcopyrite intergrown with pentlandite (sample MOX14). In reflected light, plane polarised light, in oil.

8.1.2 Recrystallized gabbronorite

The unit is characterised by up to 5 vol. % sulphides and up to 4 vol. % of oxides (magnetite and ilmenite) plus minor chromite. The sulphides are pyrrhotite (0 – 75 %), chalcopyrite (25 – 40 %), pentlandite (10 – 20 %) and pyrite (0 – 35 %). Texturally, the sulphides occur as

i) disseminations of small composite or monomineralic grains included in, or interstitial to, recrystallized silicate grains (mostly orthopyroxene), and

ii) replacements of primary silicates along cleavage planes in the form of fine disseminations intergrown with the alteration minerals.

Pyrrhotite forms micron- to millimetre-sized grains that are often intergrown with chalcopyrite and pentlandite and may carry flame-like exsolution lamellae of the latter (Fig. 8.2a). The mineral rarely forms monomineralic grains.

Chalcopyrite occurs as an interstitial phase that is internally homogenous and has irregular grain margins. It is commonly intergrown with pentlandite and pyrrhotite, in places forming lamellae in pyrrhotite (Fig. 8.2a and b). It also replaces pyrrhotite along fractures (Fig. 8.2e) and orthopyroxene along cleavage planes. Secondary minerals after plagioclase and pyroxenes (i.e. chlorite, amphibole, quartz and albite) with disseminated (a few µm sized) chalcopyrite and, in places, pyrite form an aureole around composite sulphides or monomineralic chalcopyrite (Fig. 8.2c and d). Finally, chalcopyrite may be included in plagioclase as monomineralic anhedral grains (Fig. 8.2c), or intergrown with minor pyrite (Fig. 8.2d).

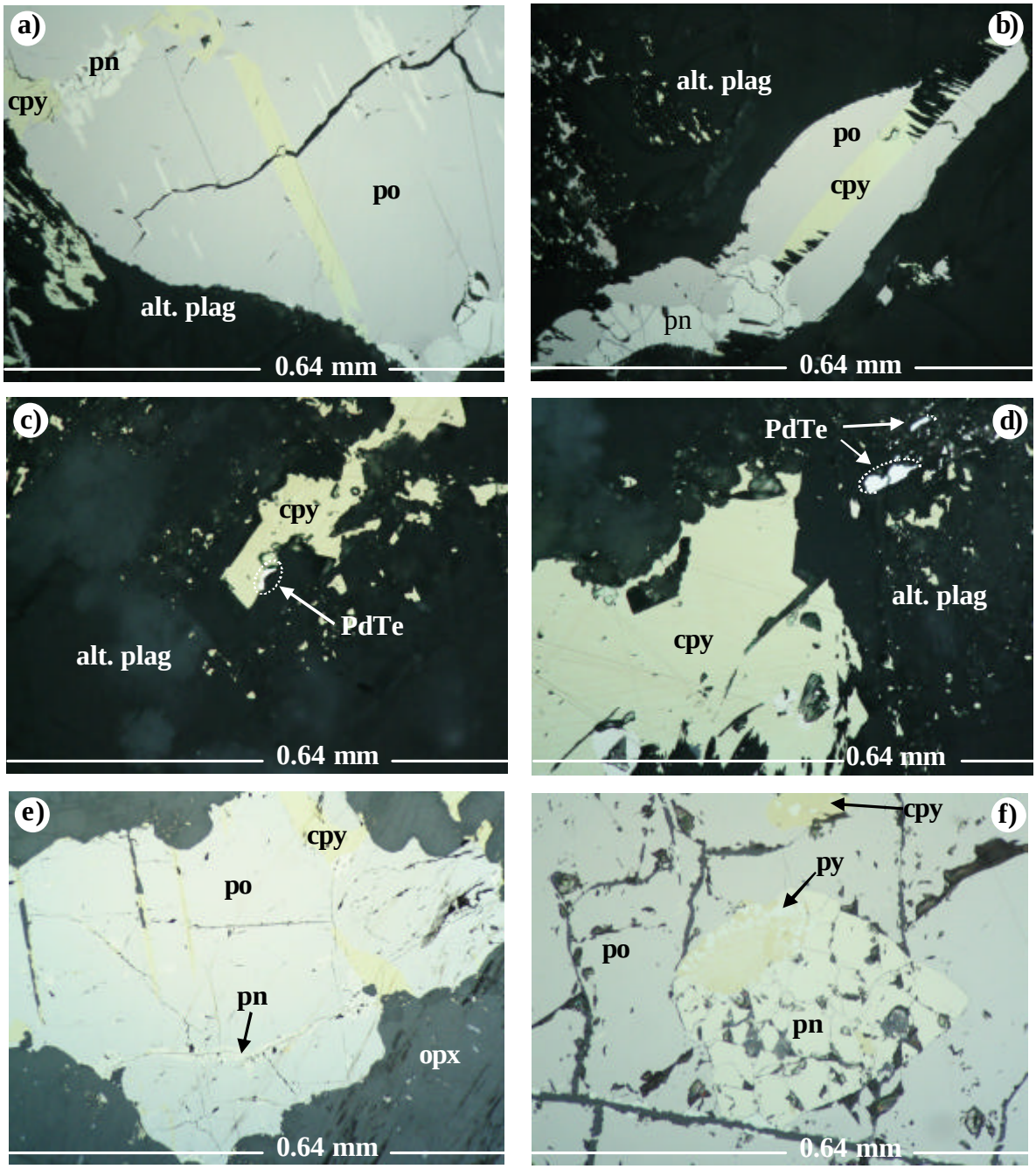

Fig. 8.2: Photomicrographs:
(a & b) Pyrrhotite (po) intergrown with minor chalcopyrite (cpy) and pentlandite (pn). Note the pentlandite and chalcopyrite lamellae in pyrrhotite (sample MOX12). (c & d) Anhedral chalcopyrite with an aureole of disseminated chalcopyrite intergrown with alteration silicate minerals (mainly chlorite after plagioclase) (sample MOX9). (e) Anhedral pyrrhotite intergrown with pentlandite along fractures and chalcopyrite along its margins (sample MOX12). (f) Fractured pyrrhotite enclosing fragmented, vaguely round pentlandite that is intergrown with pyrite (py) and chalcopyrite on its margin. Note also chalcopyrite enclosed in pyrrhotite (sample MOX10). In reflected light, plane polarised light, in oil.

Pentlandite forms flame-like exsolution lamellae and granular masses included in pyrrhotite (Fig. 8.2f) or along pyrrhotite grain margins and fractures (Figs. 8.2b and e, respectively). Pentlandite included in pyrrhotite may be intergrown with worm-like intergrowths of chalcopyrite and pyrite at its margin (Fig. 8.2f), suggesting replacement of pentlandite by chalcopyrite and pyrite. Other forms of pentlandite-chalcopyrite-pyrite intergrown are shown in Fig. 8.2g and h.

Pyrite occurs predominantly as polycrystalline fracture fillings in plagioclase (Fig. 8.2i and j) and, in places, as rims around pentlandite, in which case it may be intergrown with chalcopyrite (Fig. 8.2g).

Ilmenite (up to 400 µm) occurs interstitial to, or included in, pyroxene. The grains are anhedral, internally homogenous and often intergrown with magnetite (Fig. 8.2k). Magnetite is also interstitial and, as mentioned above, is mostly intergrown with ilmenite grains. Magnetite may be replaced by pyrrhotite along cleavage planes (Fig. 8.2k).

Notably, samples with high pyrrhotite contents contain no pyrite and vice versa. This suggests a reaction-replacement relationship between the two sulphides. The presence of pyrite may suggest increased S fugacity (fS_2) resulting in pyrrhotite being replaced by pyrite.

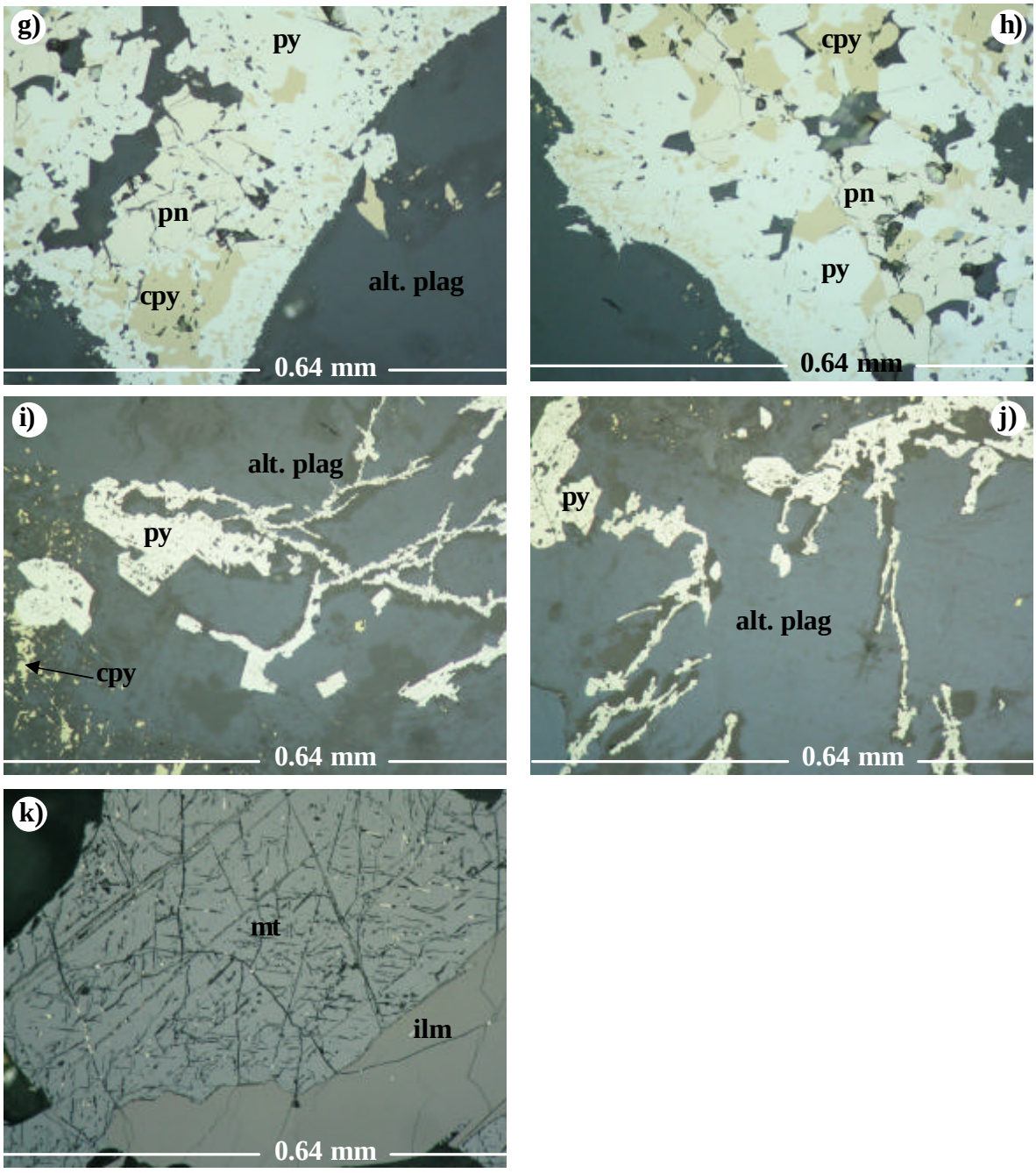

Fig. 8.2 continued. Photomicrographs:
(g & h) Pyrite enclosing fragmented pentlandite and intergrown with disseminated chalcopyrite. Note the rim of fine chalcopyrite intergrown with pyrite around the coarse, fragmented, composite sulphide (sample MOX10), (i & j) Pyrite in fractures within altered plagioclase (alt. plag). Disseminated chalcopyrite is intergrown with secondary silicates (sample MOX9 and 10, respectively). (k) Magnetite (mt) intergrown with ilmenite (ilm). Magnetite contains pyrrhotite along cleavage planes (sample MOX12). In reflected light, plane polarised light, i and j in air and g, h and k in oil.

8.1.3 Anorthosite

The anorthosites may contain up to 20 vol. % sulphides, in relative proportions: chalcopyrite 35 – 85 %, pyrrhotite 5 – 50 %, pentlandite 5 – 20 %, and pyrite 0 – 15 %. Up to 3 vol. % ilmenite with rare magnetite and chromite may also occur. The sulphides tend to be associated with felsic domains of the rock and the relative proportions of the sulphides are extremely variable ranging from chalcopyrite-dominated to pyrrhotite-dominated. Chalcopyrite-dominated samples have the highest sulphide contents. The sulphides occur as

i) aggregates of composite grains interstitial to plagioclase and clinopyroxene or included in clinopyroxene, and
ii) replacement minerals along cleavage planes of clinopyroxene, fractures in plagioclase or intergrown with secondary alteration silicates.

Two generations of chalcopyrite are present in the samples.

(1) The first occurs as irregular shaped, mostly fractured interstitial monomineralic grains that range from a few µm to mm in size. In places, the chalcopyrite grains are corroded and intergrown with secondary silicate minerals (amphiboles), mostly along grain boundaries. The chalcopyrite may include coarse (mm-sized) subhedral crystals of pyrite, small (1 – 2 µm) crystals of sphalerite and pyrrhotite as well as zircon (Fig. 8.3a), apatite and calcite. Zircon and apatite are euhedral or subhedral in shape and up to 100 µm and 1-2 µm in size, respectively.

(2) The other generation of chalcopyrite is of a secondary nature and occurs as

i) rims around pyrrhotite which in turn is rimmed by secondary pyrite (Fig. 8.3b and c), and

ii) vaguely round vermicular intergrowths of chalcopyrite and pyrite included in pyrrhotite (Fig. 8.3d and e).

Pyrrhotite mostly occurs as interstitial anhedral grains that are intergrown with chalcopyrite and pentlandite (Fig. 8.3f). Pyrrhotite also includes vaguely round vermicular intergrowths of pyrite and chalcopyrite, in places with a remnant of pentlandite (Fig. 8.3d and e, respectively). Similar textural intergrowths have been observed in recrystallized gabbronorite of the Platreef (Section 7.1.2) and in the Main Sulphide Zone of the Great Dyke of Zimbabwe (Oberthür, personal communication, 2005), where these textures were interpreted as replacements of pentlandite by pyrite and chalcopyrite.

Pentlandite occurs as fragmented interstitial grains that may be intergrown with chalcopyrite (Fig. 8.3g), as fracture fillings together with pyrite, pyrrhotite and chalcopyrite, along grain margins in pyrrhotite, or as minor flame- like exsolution lamellae and vaguely round inclusions in pyrrhotite. In places, pentlandite may be altered and replaced by coronas of violarite (Fig. 8.3h). Relict pentlandite forming islands in violarite is observed in sample MOX29 (Fig. 8.3i).

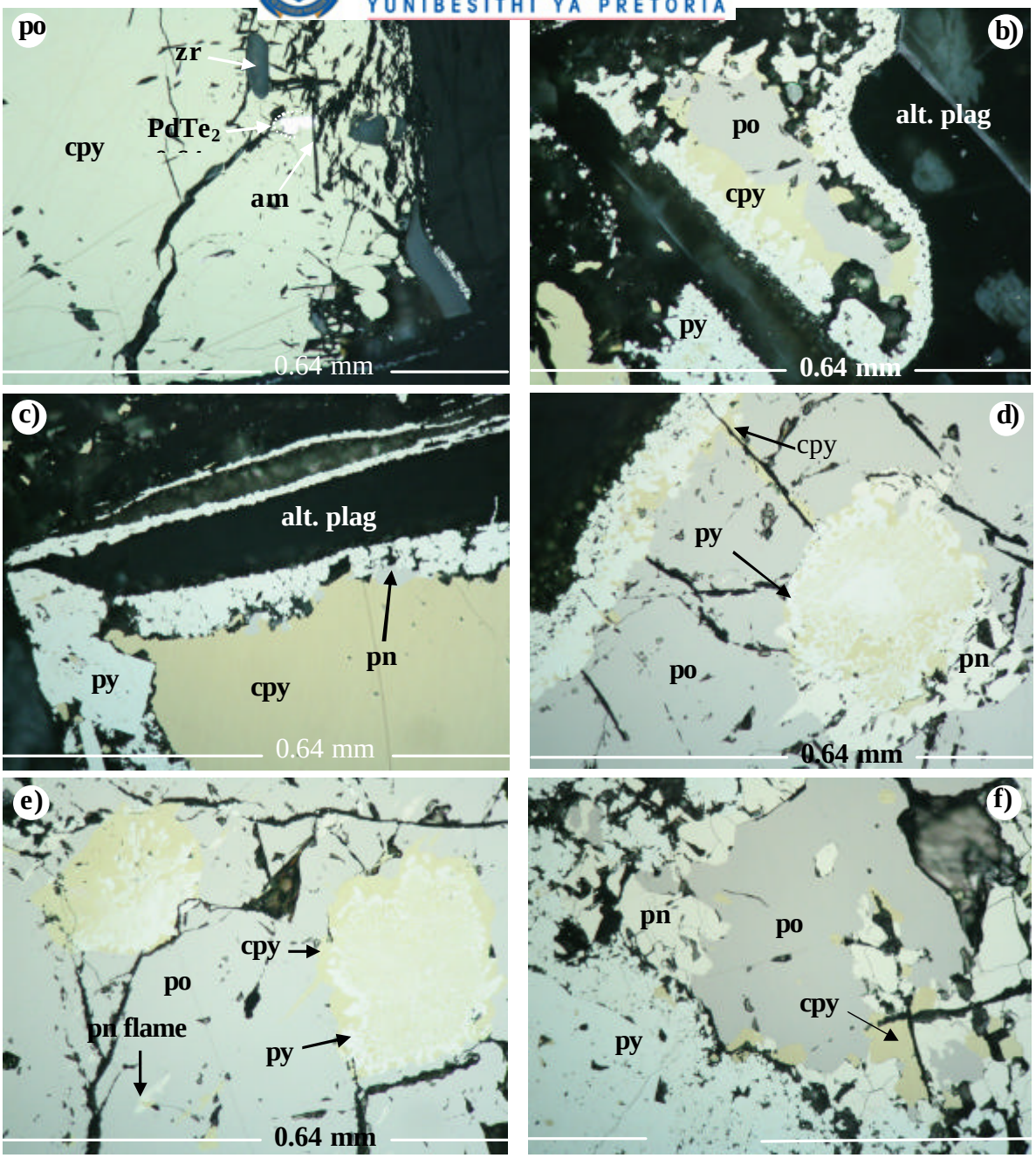

Fig. 8.3: Photomicrographs:
(a) Chalcopyrite intergrown with amphibole (am) laths along its margin, and enclosing subhedral zircon (sample MOX29). (b) Aggregate of pyrrhotite rimmed by chalcopyrite which is in turn rimmed by pyrite (sample MOX32). (c) Chalcopyrite intergrown with minor pentlandite at its margin and rimmed by pyrite. Note streaks of pyrite in adjacent altered plagioclase (Sample MOX32). (d) Pyrrhotite enclosing an intergrowth of pentlandite, pyrite and chalcopyrite. The corona around pyrrhotite consists of pyrite intergrown with minor chalcopyrite (sample MOX32). (e) Pyrrhotite enclosing vaguely round blebs of an intergrowth of pyrite and chalcopyrite. Chalcopyrite is concentrated towards the rims whereas pyrite is concentrated in the core. Pyrrhotite additionally contains flame-like exsolutions of pentlandite (sample MOX32). (f) Intergrowth of pyrrhotite (po) pyrite (py), minor chalcopyrite (cpy), and pentlandite (pn). (sample MOX27). opx = orthopyroxene. In reflected light, plane polarised light, in oil.

Pyrite exhibits a wide variety of textures. The main modes of occurrence are:

i) worm-like intergrowths with chalcopyrite and pyrrhotite (Fig. 8.3d)

ii) deuteric veinlets within plagioclase (Fig. 8.3c)

iii) replacement of clinopyroxene along cleavage planes and fractures (Fig. 8.3l).

In addition, pyrite occurs as an interstitial phase along plagioclase and clinopyroxene grain margins where, in places, it may replace the silicate minerals (Fig. 8.3j and k). It can also occur along plagioclase and clinopyroxene cleavage planes (Fig. 8.3l), or cross-cutting quartz. In the latter case it is net textured and porous and often intergrown with minor chalcopyrite.

Ilmenite is interstitial to, or enclosed in, pyroxenes. Most of the grains are altered to leucoxene suggesting fluid activity. Hematite tends to be euhedral, up to 1 mm in size, and occurs included in chalcopyrite. Rare magnetite, containing ilmenite lamellae, occurs interstitial to silicates or enclosed in altered orthopyroxene.

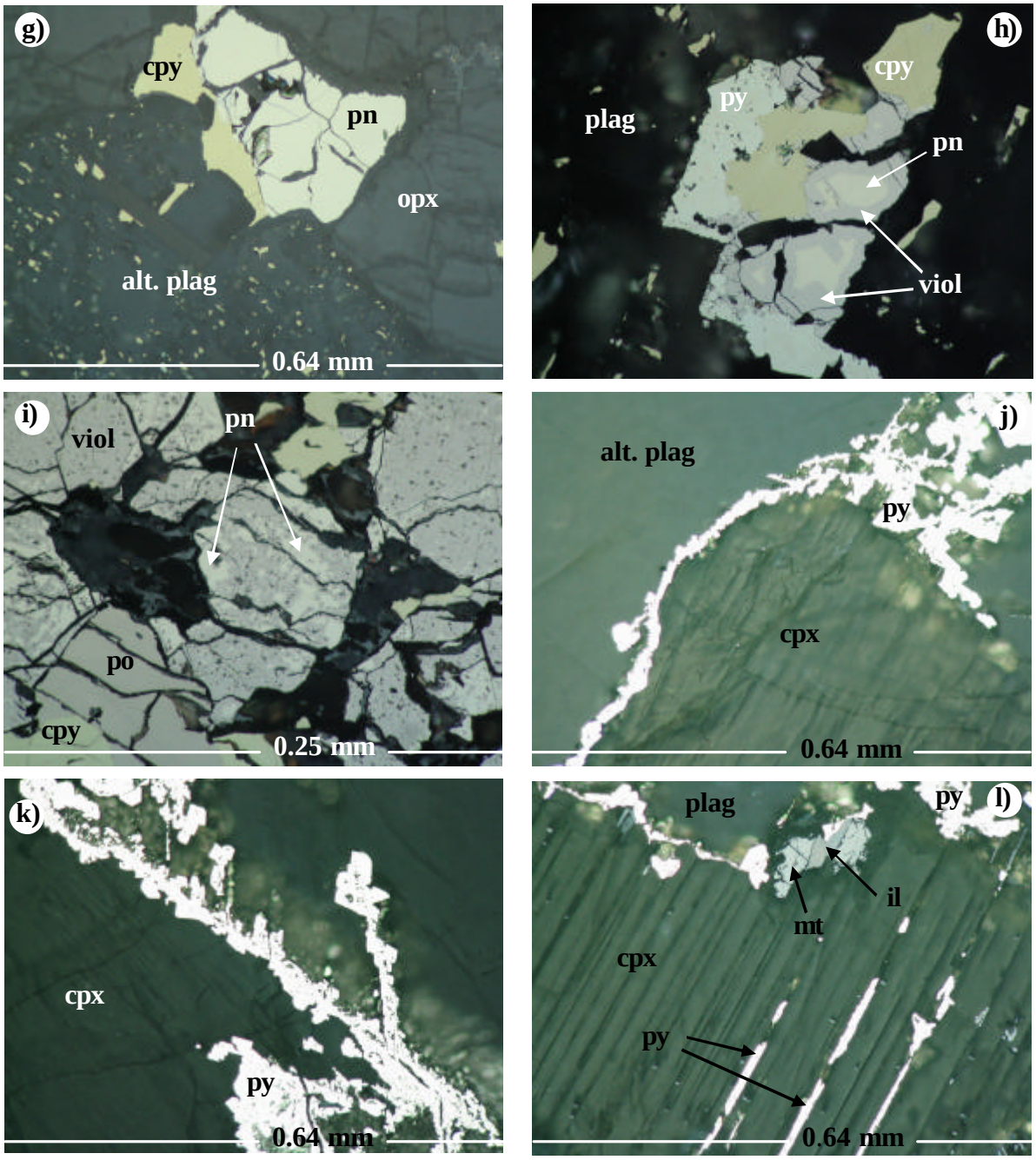

Fig. 8.3 continued:
(g) Interstitial pentlandite intergrown with chalcopyrite. Disseminated chalcopyrite replaces adjacent altered plagioclase (alt. plag) along cleavage planes (sample MOX27). (h) Violarite (viol) rimming pentlandite and intergrown with pyrite and chalcopyrite sample (MOX29). (i) Violarite with minor relictic pentlandite is intergrown with pyrrhotite and chalcopyrite (sample MOX29). (j & k) Pyrite occurs interstitial to plagioclase and clinopyroxene (cpx) and replaces the silicates along fractures (sample MOX32). (l) Interstitial pyrite replaces clinopyroxene along cleavage planes (sample MOX 32). In reflected light, plane polarised light, in oil.

8.2 Sulphide and oxide minerals on Townlands

8.2.1 Upper Platreef

The Upper Platreef is characterised by low sulphide contents (< 2 vol. %) towards the top of the Unit, and sulphide-rich rocks (up to 30 vol. %) towards the base. The latter may also contain up to 5 vol. % oxides (chromite, magnetite and ilmenite). The sulphide assemblage consists of pyrite (30 – 70 %), chalcopyrite (15 -50 %) and millerite (0 – 20 %). Pyrrhotite is rare. Only one sample (P2) contained abundant pentlandite (60 %) in addition to chalcopyrite (15 %). Minor amounts of violarite and covellite are also present in the rocks.

It is important to note that the samples with low sulphide contents have the lowest pyrite and highest chalcopyrite contents, whereas the sulphide-rich samples near the base of the Unit have high pyrite and low chalcopyrite contents and always contain millerite. The dominance of pyrite towards the basal portions of the Platreef was also reported by Iljina and Lee (2005). This was interpreted to suggest a change from S-rich to S-poor (or metal rich) environments during the crystallisation of the Platreef.

Pyrite occurs as massive, up to 10 mm-wide subhedral or anhedral grains that are mostly intergrown with chalcopyrite and secondary silicates (mainly amphiboles; (Fig. 8.4a and b). Coarse pyrite is often cut by veinlets of intergrown millerite and chalcopyrite (Fig. 8.4e and f). Locally, pyrite is intergrown with magnetite that encloses, or is intergrown with, millerite and fine chalcopyrite (Fig. 8.4c and d).

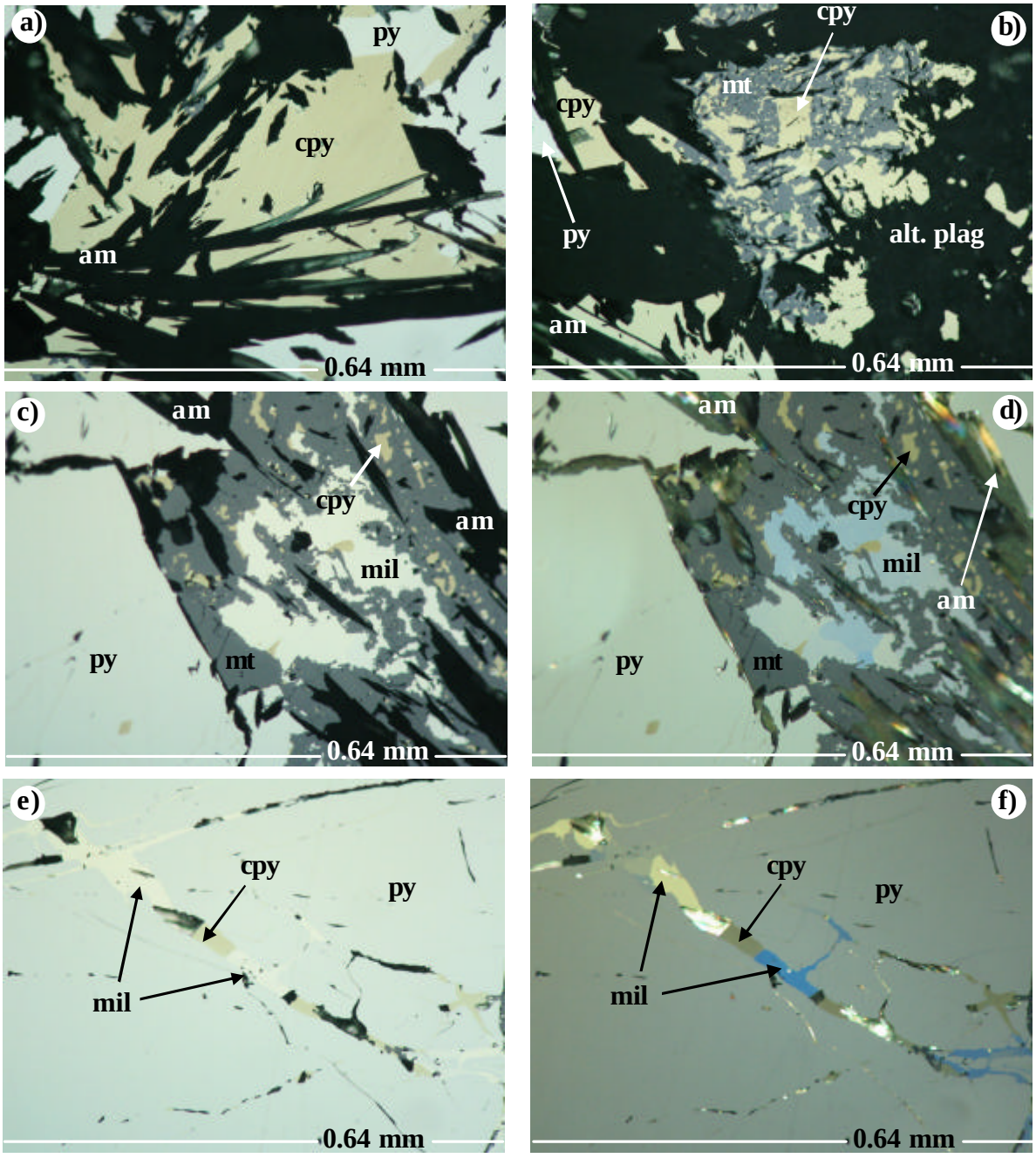

Fig. 8.4: Photomicrographs:
(a) Chalcopyrite (cpy) and pyrite (py) intergrown with acicular amphibole actinolite (am) (sample P7). (b) An aggregate of intergrown anhedral magnetite (mt) and chalcopyrite in altered plagioclase (alt. plag) (sample P7). (c & d) Coarse pyrite intergrown with magnetite that encloses millerite (mil). Magnetite is also intergrown with anhedral, disseminated chalcopyrite (sample P7). (e & f) Coarse pyrite cut by veinlets of intergrown chalcopyrite and millerite (sample P7). In reflected light, in oil, (a, b & e) plane polarised light and (d & f) cross polarised light.

Chalcopyrite exhibits a variety of textures. It occurs as coarse (up to 1.5 mm) grains that are intergrown with pyrite and acicular (up to 1.5 mm) amphibole (actinolite) (Fig. 8.4a). It also occurs as disseminated anhedral grains intergrown or enclosed in magnetite (Fig. 8.4b, c and d) and intergrown with millerite along fractures in coarse pyrite (Fig. 8.4e and f). Coarse interstitial chalcopyrite grains which may be intergrown with minor pentlandite on their margins occur in places and are cut and replaced by covellite veinlets and rimmed by magnetite (Fig. 8.4g and h). Patchy chalcopyrite grains occur along the margins of anhedral violarite masses after pentlandite (Fig. 8.4i).

Millerite is anhedral and occurs intergrown with chalcopyrite in fractures within coarse pyrite (Fig. 8.4e and f) or enclosed in magnetite (Fig. 8.4b end c).

Pentlandite tends to be intergrown with chalcopyrite and is often cut by veinlets of magnetite and minor covellite. In places, pentlandite forms minor anhedral grains at the margins of violarite (Fig. 8.4i and j).

Violarite forms anhedral, patchy masses that are intergrown with chalcopyrite and associated with magnetite along its margins (Fig. 8.4i and j). As noted earlier, minor amounts of pentlandite may occur along the margins of violarite, suggesting that the pentlandite is relictic and that most of the primary pentlandite has been replaced by violarite.

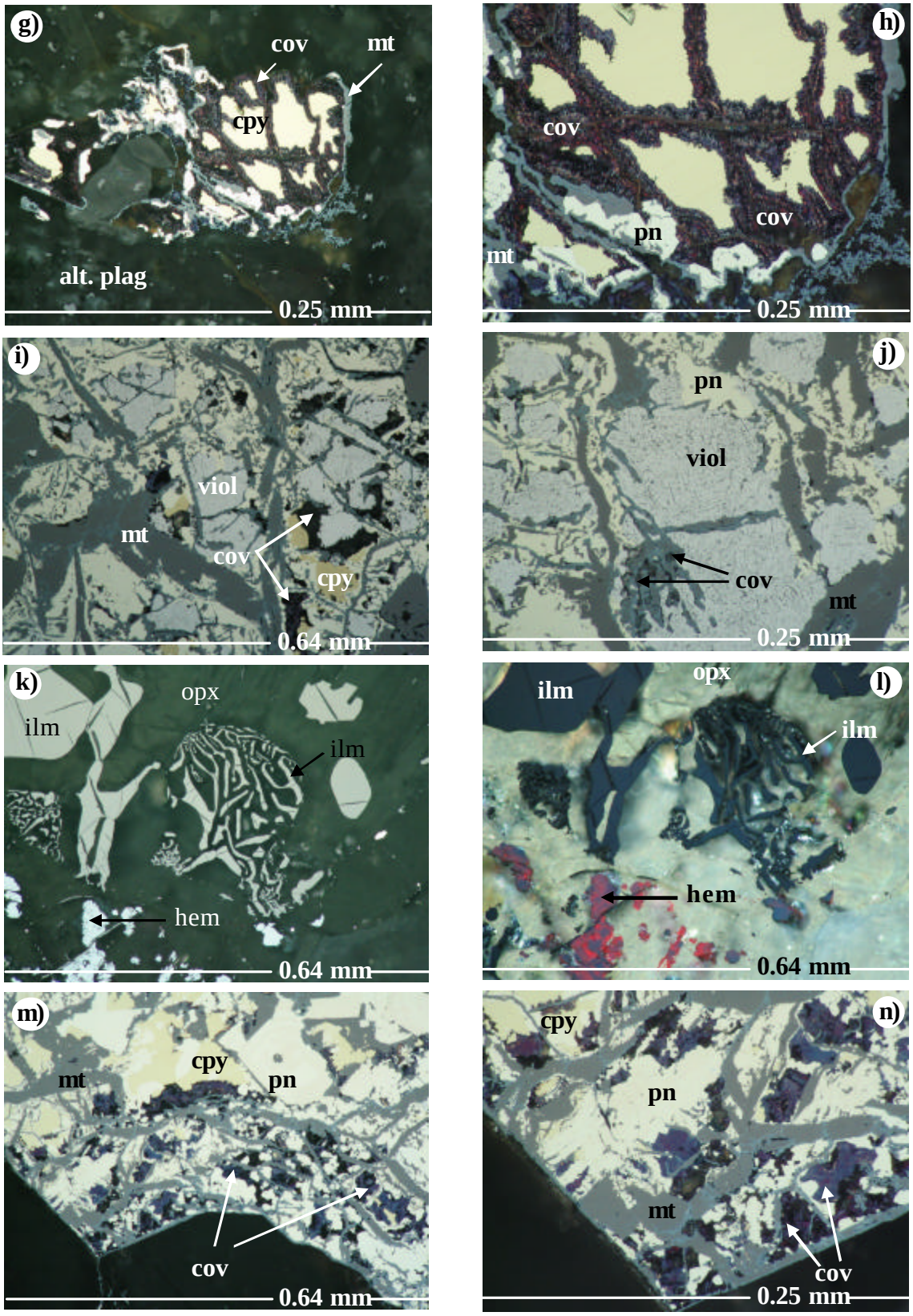

Fig. 8.4 continued: Refer to next page for explanation of the photomicrographs

Fig. 8.4 continued:
g & h) Chalcopyrite cut by covellite (cov) veins and rimmed by magnetite. Note minor pentlandite in h (sample P2). (i & j) Patches of violarite intergrown with pentlandite, minor chalcopyrite, covellite and cut by magnetite veinlets (sample P2). (k & l) Intergrowth of orthopyroxene (opx) and ilmenite, as well as granular, subhedral and anhedral ilmenite (ilm), orthopyroxene (opx) and minor anhedral hematite (hem) (sample P4). (m & n) Pentlandite and chalcopyrite show extensive alteration to covellite and magnetite along irregular fractures (sample P2). In reflected light, plane polarised light except l, in oil.

Covellite replaces chalcopyrite along fractures (Fig. 8.4g and h) or forms islands towards altered margins of composite sulphides where it is associated with magnetite (Fig. 8.4m and n).

Magnetite is anhedral and may be intergrown with anhedral disseminated chalcopyrite or it may enclose an intergrowth of anhedral millerite and chalcopyrite grains (Fig. 8.4b and d, respectively). Ilmenite is internally homogenous, forming anhedral or subhedral grains that may be included in orthopyroxene or occur as intergrowth of ilmenite and orthopyroxene (Fig. 8.4k and l). Anhedral hematite (oxidised magnetite) enclosed in plagioclase was also identified and is mostly associated with ilmenite (Fig. 8.4k and l).

8.2.2 Middle Platreef

As the Upper Platreef, the Middle Platreef is also characterised by an inhomogeneous distribution of the sulphides. The samples towards the top of the unit have 1 – 2 vol. % sulphides whereas those towards the base have 15 – 20 vol. % sulphides. The proportions of the different sulphides show significant variation especially in samples with low sulphide contents. Some samples are pyrrhotite-rich (up to 70 %) and contain no pyrite, whereas others are pyrite-rich

(up to 75 %) with only minor to trace amounts of pyrrhotite. Chalcopyrite and pentlandite occur in about equal amounts and together constitute 20 – 30 % of the sulphides. Samples with high sulphide contents are characterised by abundant pyrite (50 – 60 %), as well as millerite (10 – 20 %), chalcopyrite (10 – 20 %) and pentlandite (0 – 20 %). Trace amounts of galena and rare molybdenite are also present, but pyrrhotite is absent. Oxides reach a maximum of 4 vol. % and include magnetite, chromite and ilmenite.

Pyrite exhibits a variety of textures. It occurs as polycrystalline monomineralic grains up to 5 mm in size or as net-textured or vermicular masses in plagioclase (Fig. 8.5a and b). It may also occur as a replacement sulphide in fractures in altered pyroxene (Fig. 8.5b). In places, pyrite occurs as rims around chalcopyrite or millerite (Fig. 8.5a and e, respectively) or in millerite-bearing veinlets that transect through chalcopyrite (Fig. 8.5f and g). Pyrite may be cut by polycrystalline veinlets containing intergrown chalcopyrite and pentlandite (Fig. 8.5c and d).

Chalcopyrite occurs as optically homogenous grains with irregular grain margins, often intergrown with magnetite (Fig. 8.5h) and pyrite (Fig. 8.5i). Chalcopyrite may be interstitial to millerite (Fig. 8.5j) and in places enclosing millerite (Fig. 8.5k), or it may occur at the margin of intergrown millerite and pyrite (Fig. 8.5l and m). As noted earlier, chalcopyrite may be transected by millerite veinlets (Fig. 8.5f and g). The coarse grains of chalcopyrite occasionally display twinning (Fig. 8.5j and k). Fine disseminated chalcopyrite grains also occur around pyrite or magnetite (Fig. 8.5h), or are remobilised together with pentlandite along veinlets that cut through plagioclase (Fig. 8.5d).

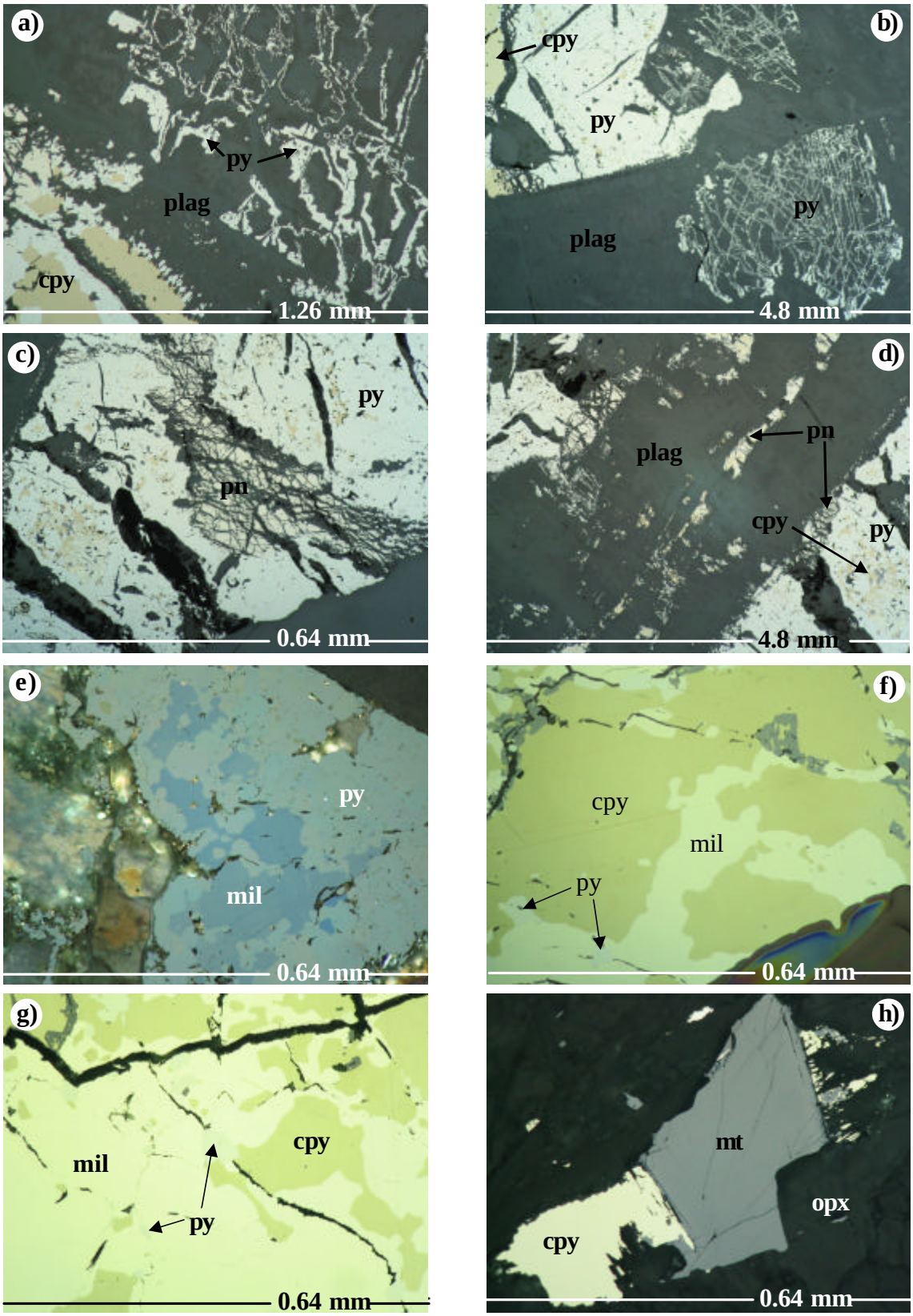

Fig. 8.5: Refer to next page for explanation of the photomicrographs.

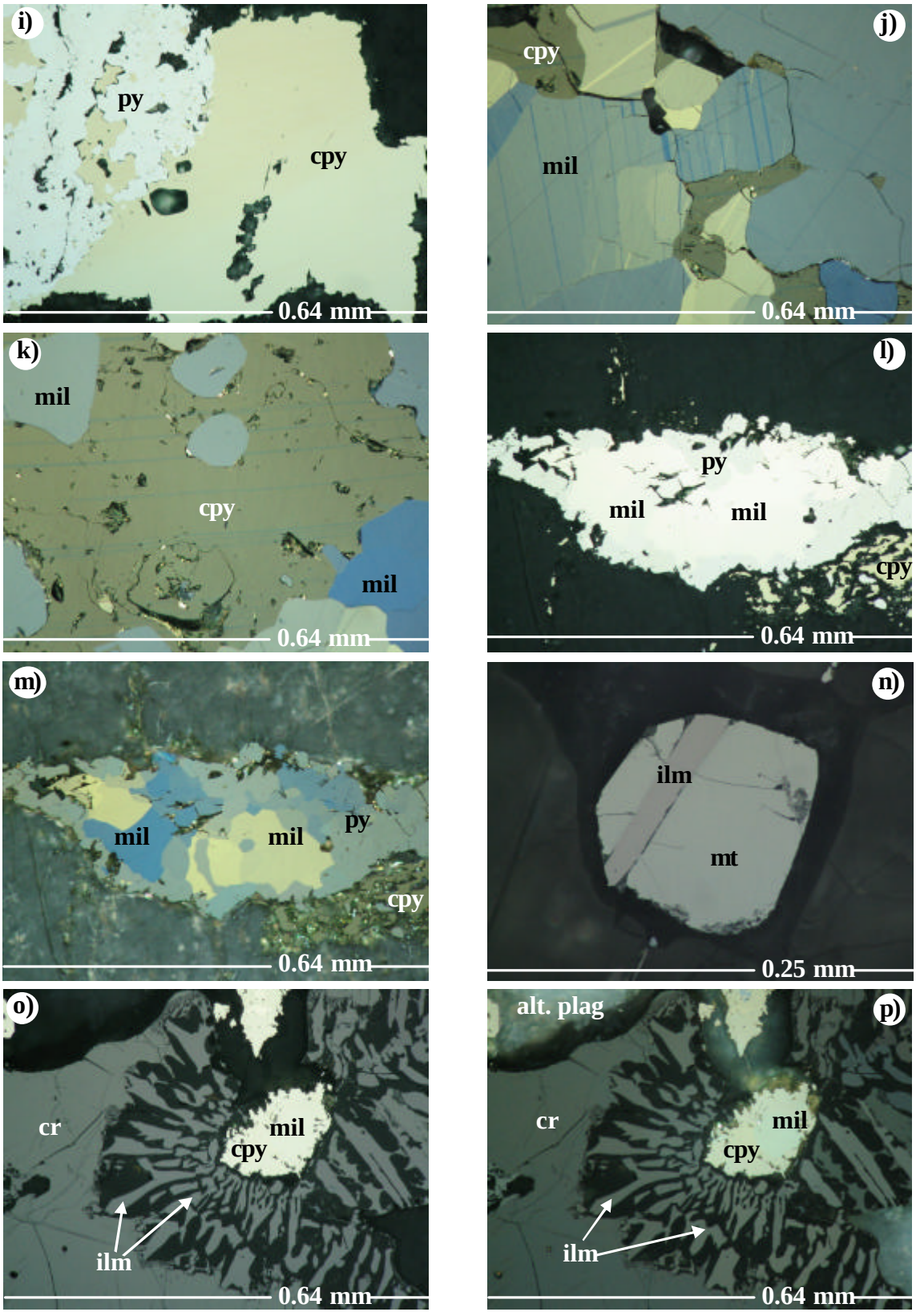

Fig. 8.5 continued: Refer to next page for explanation of the photomicrographs.

Fig. 8.5: Photomicrographs:

(a) Plagioclase (plag) containing vermicular network of pyrite. Pyrite also forms coronas around chalcopyrite (sample P19). (b) Skeletal pyrite and pyrite replacing plagioclase along cleavage planes (sample P19). (c) Pyrite cut by pentlandite-rich veins. Also note fine disseminated chalcopyrite in pyrite (sample P19). (d) Pentlandite replacing plagioclase along cleavage planes. Matrix is pyrrhotite with disseminated fine chalcopyrite (sample P19). (e) Pyrite enclosing millerite. Note fine disseminated chalcopyrite intergrown with pyrite (sample P15). (f & g) Millerite replacing chalcopyrite along fractures. Minor pyrite (py) grains occur at the contact between chalcopyrite and millerite, or are enclosed in millerite (sample P14). (h) Magnetite (mt) is intergrown with chalcopyrite, with minor chalcopyrite being remobilised into adjacent silicates (sample P11). In reflected light, cross polarised light, in oil.

Fig. 8.5 continued:

(i) Anhedral chalcopyrite intergrown with anhedral pyrite (sample P11). (j) Massive, twinned, subhedral millerite (mil) intergrown with interstitial chalcopyrite (cpy) (sample P106). (k) Anhedral, twinned chalcopyrite intergrown with, and enclosing, vaguely round millerite (sample P106). (l & m) Fragmented pyrite intergrown with millerite and chalcopyrite (sample P15). (n) Subhedral magnetite with ilmenite lamellae (sample P15). (o & p) Radiating, skeletal ilmenite vaguely round chromite (cr) and enclosing an intergrowth of chalcopyrite and millerite (sample P15). In reflected light, plane polarised light (except i, l, n and o), in oil.

Millerite occurs as massive, subhedral or anhedral grains that may form monomineralic aggregates, in places intergrown with chalcopyrite and pyrite (Fig. 8.5j, k and e), or as veins in fractured chalcopyrite (Fig. 8.5f and g). The grains show distinct pleochroism from yellowish cream to bluish grey/cream in reflected light and abundant internal lamellae. Millerite may also be rimmed by pyrite (Fig. 8.5l and m).

Magnetite is euhedral to subhedral and occurs interstitial to, or enclosed, in pyroxenes. It often contains thick lamellae of ilmenite (Fig. 8.5n).

Chromite is subhedral and optically homogenous. It may occur surrounding radiating skeletal ilmenite grains that in turn surround composite grains of chalcopyrite and millerite (Fig. 8.5o and p).

8.3 Compositions of major base metal sulphides and spinel

Pentlandite, pyrrhotite, pyrite and chalcopyrite were analyzed by microprobe, both in the "normal" analytical mode and using the TRACE program (35 kV voltage; high current, extended counting times of up to 10 minutes peak and background). The latter setup leads to detection limits of *ca.* 20 ppm Pd in pentlandite. Analytical results are given in Table 3. For the analyses, sulphides were selected from well mineralized samples of the Platreef at Nonnenwerth and Townlands, notably the recrystallized gabbronorite and anorthosite at Nonnenwerth and the Middle and Upper Platreef at Townlands.

8.3.1 Pentlandite

Pentlandite is characterised by Ni/Fe ratios close to unity (Table 3a). Cobalt contents are between 0.9 and 1.3 wt. %; only sample MOX12 has a higher Co content (1.7 to 1.8 wt. %). Notably, there is considerable variation in Co contents between samples but little intra-sample variation.

There is a dramatic difference in the Pd contents of pentlandite from Nonnenwerth and Townlands.

Up to 700 ppm Pd were analyzed in pentlandite from Nonnenwerth; samples from recrystallized gabbronorite contain the highest Pd contents (139 – 697 ppm, averaging 433 ppm) whereas samples from anorthosites have generally between 66 – 224 ppm (average 147 ppm).

In the "typical magmatic" sulphide assemblage at Nonnenwerth, no PGM enclosed in pentlandite were identified. It is well-known that pentlandite may carry even up to some % of Pd (substituting for Ni) in its crystal lattice (e.g. Gervilla et al., 2004).

In contrast, pentlandites from Townlands have Pd contents below the detection limit (20 ppm Pd) of the method. This lack of measurable Pd contents in pentlandite may find the following explanations: (i) Pd in pentlandite was analysed in one sample (P 13) only, so the results may not be representative. (ii) The Townlands sulphide assemblage differs from being "typical magmatic" and has experienced syn- to post-magmatic modification (formation of millerite and pyrite replacing the lower-S minerals pentlandite and pyrrhotite). Therefore, the relatively rare pentlandite at Townlands may either represent a second generation of pentlandite, or is a relict phase that has suffered an overprint that extracted earlier lattice-bound Pd. (iii) Pd-bearing PGM could have been mobilized during replacement of 'primary' sulphides by pyrite dominated assemblages into the surrounding silicates (Prichard *et al*., 2001).

The analytical work presented here has shown marked differences in Pd contents in pentlandites from the Platreef for the first time. It is suggested that systematic

research in this topic would be a worthwhile undertaking to further our understanding of the distribution of the PGE in Platreef ores.

Se contents vary between 200 – 500 ppm (averaging 282 ppm) in Nonnenwerth samples, and 70 – 450 ppm (averaging 173 ppm) at Townlands. Rhodium, platinum and silver are below the detection limits of the electron microprobe.

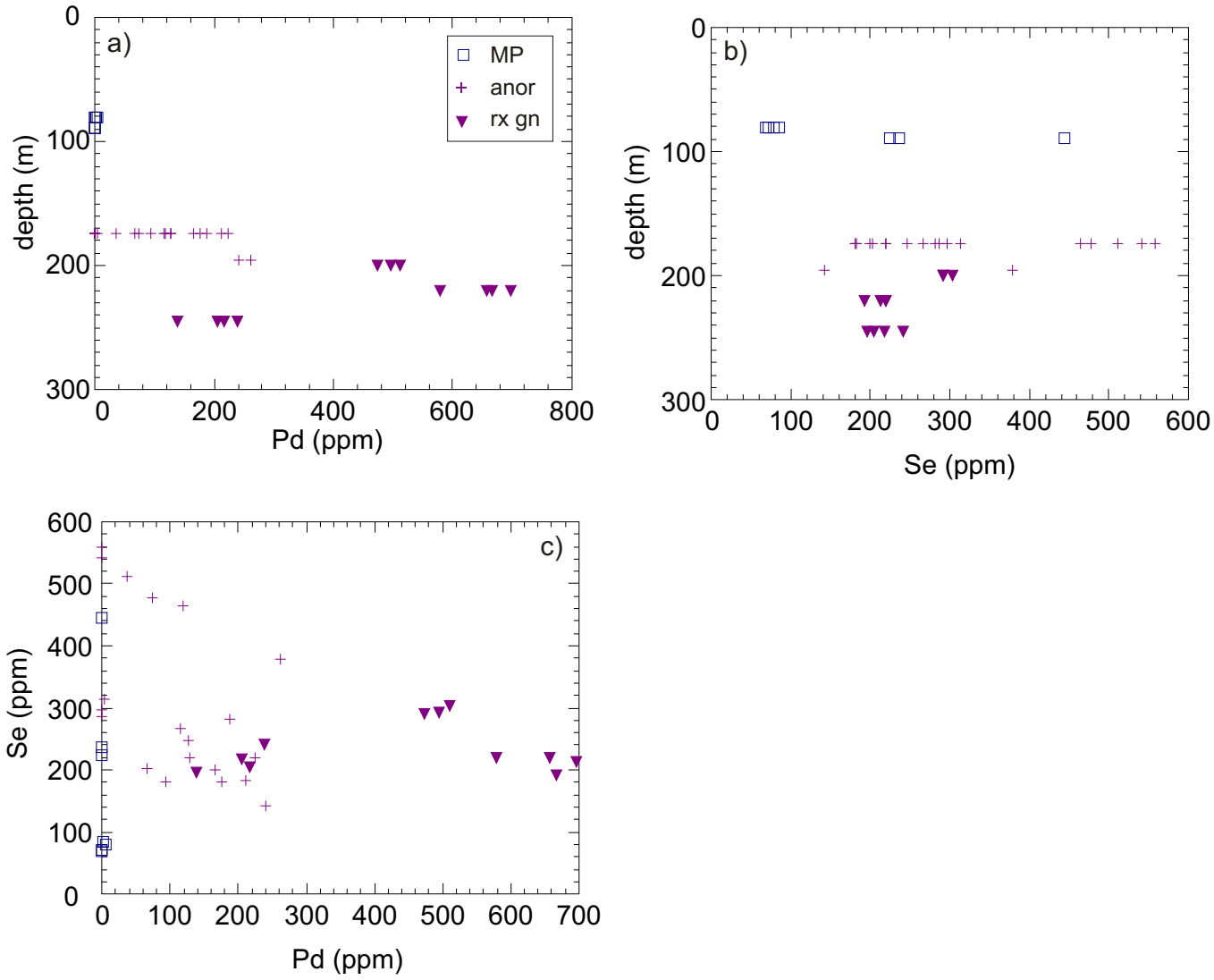

Fig. 8.6:Variation of a) Pd, b), Se with depth in pentlandite, andSe versus Pd. MP = Middle Platreef (from Townlands), anor = anorthosite, rx gn = recrystallized gabbronorite (both from Nonnenwerth).

8.3.2 Pyrrhotite

Pyrrhotite has between 47 – 48.5 atomic % Fe and 51.2 – 52.8 atomic % S indicating the presence of hexagonal/monoclinic pyrrhotite ($Fe_{1-x}S$) (Table 3b). Se contents range from 216 – 362 ppm (averaging 267 ppm) in Nonnenwerth samples and 38 – 128 ppm (averaging 98 ppm) at Townlands. Fe and S show distinct differences between samples but little within sample variation. Pyrrhotite from Nonnenwerth anorthosite has the highest Fe (48.1 – 48.4 atomic %), followed by pyrrhotite from the recrystallized gabbronorite (47.3 – 47.6 at. %), with the Townlands pyrrhotites (both from the Upper and Middle Platreef) having the lowest Fe contents (46.9 – 47.1 at. %). Pyrrhotites from recrystallized gabbronorite and anorthosite have generally similar Se contents, and no PGE were detected. Pt, Pd and Rh contents are all below the detection limits of the electron microprobe.

8.3.3 Pyrite

Platreef pyrite is characterised by stoichiometric Fe and S contents (Table 3c). Pyrite from Nonnenwerth samples carries no Co but up to 1 wt. % Ni is present in pyrite from anorthosite samples. Pyrite from Townlands is Co- and Ni- bearing, with up to 1.8 wt. % Co and 1 wt. % Ni. Pt, Pd and Rh contents are all below the detection limits of the electron microprobe. Se contents of pyrite vary from 104 – 377 ppm (average 224 ppm) in recrystallized gabbronorite, and 143 – 327 ppm (average 266 ppm) in anorthosite, with one sample (MOX29) having 720 ppm Se. Townlands pyrite has 31 to 338 ppm Se with a generally similar range for the Upper and Middle Platreef. No systematic compositional variation of pyrite with depth or lithology is visible at Townlands or Nonnenwerth.

8.3.4 Chalcopyrite

Only two analyses of chalcopyrite from Nonnenwerth recrystallized gabbronorite (sample MOX10) were obtained. Chalcopyrite has a stoichiometric composition with PGE, Ni, Au, Co, Se and Ag levels below the detection limit suggesting that none of these elements substitute significantly in chalcopyrite (Table 3d).

8.3.5 Millerite

One analysis each of millerite from the Upper Platreef and Middle Platreef on Townlands were obtained. Millerite has a stoichiometric composition with significant Fe (<1.6 wt. %).

8.3.6 Spinel

Spinel-group minerals resembling chromite in reflected light are accessory minerals in serpentinised peridotite and some high magnesian gabbronorites from Nonnenwerth. Analytical results for “chromite” (more precise: Cr-bearing magnetite; see below), corrected for Fe^{3+} content using the method of Finger (1972), are given in Table 4. However, the compositional variations and trends of the chromites are difficult to comment on because only a small number of grains were observed and analysed (8 grains altogether).

In the northern lobe, chromite distribution is sporadic and is mostly accessory except at few localities like Zwartfontein (Schürmann et al., 1998), Rooipoort (Maier et al., in preparation) and Grasvally (Hulbert, 1983). The stratiform-type chromites from the Lower and Critical Zones of the Rustenburg Layered Suite have the following characteristics: The LG6 layer has a Cr_2O_3 content of 46 - 47

wt. %, MG chromitites 44 - 46 wt. %, and the UG2 layer has around 43 wt. % Cr_2O_3 (Schürmann et al., 1998). The LG6 layer has a Cr/Fe ratio of between 1.56 and 1.60, MG chromitites are between 1.35 and 1.50 whilst the UG2 layer has a Cr/Fe ratio of between 1.26 and 1.40 (Schürmann et al., 1998). For Platreef chromites, Hatton and von Gruenewaldt (1987) reported Cr_2O_3 contents ranging from 34.5 up to 52.5 wt. %. On Zwartfontein, Cr/Fe ratios range from 1.13 to 2.2 (Schürmann et al., 1998).

The Cr-bearing spinels from **Nonnenwerth** have total combined iron contents ranging from 60 – 74 wt. % (FeO + Fe_2O_3) in high magnesian gabbronorite, and 71 – 78 wt. % (FeO + Fe_2O_3) in serpentinised peridotite. MgO and Al_2O_3 contents are low (ca. 1 – 3 wt. % MgO and 4 – 6 wt. % Al_2O_3). Cr_2O_3 contents are in the range 18 - 26, average 23 wt. % Cr_2O_3 in high magnesian gabbronorite, and 11 to 14, averaging 12 wt. % in serpentinised peridotite. Accordingly, Cr/Fe ratios are also low and range from 0.32 to 0.4 in serpentinised peridotite and 0.6 to 0.82 in high magnesian gabbronorite. The above analytical data clearly point to the fact that the spinels at Nonnenwerth are **Cr-bearing magnetites**.

Fig. 8.7a shows Cr # versus Fe^{2+} # of the analysed Cr-bearing magnetites. Clearly, the compositions plot outside the fields of ophiolitic and stratiform spinels/chromites, towards Fe-rich compositions (magnetite). The Cr # can still be seen to indicate a stratiform heritage, however, the Fe^{2+} # clearly points to the fact that the compositions of the Cr-bearing magnetites reflect secondary overprinting of probably primary magmatic chromites. It is well-known that Fe is released during serpentinization and may cause this observed Fe-upgrading of spinels. The

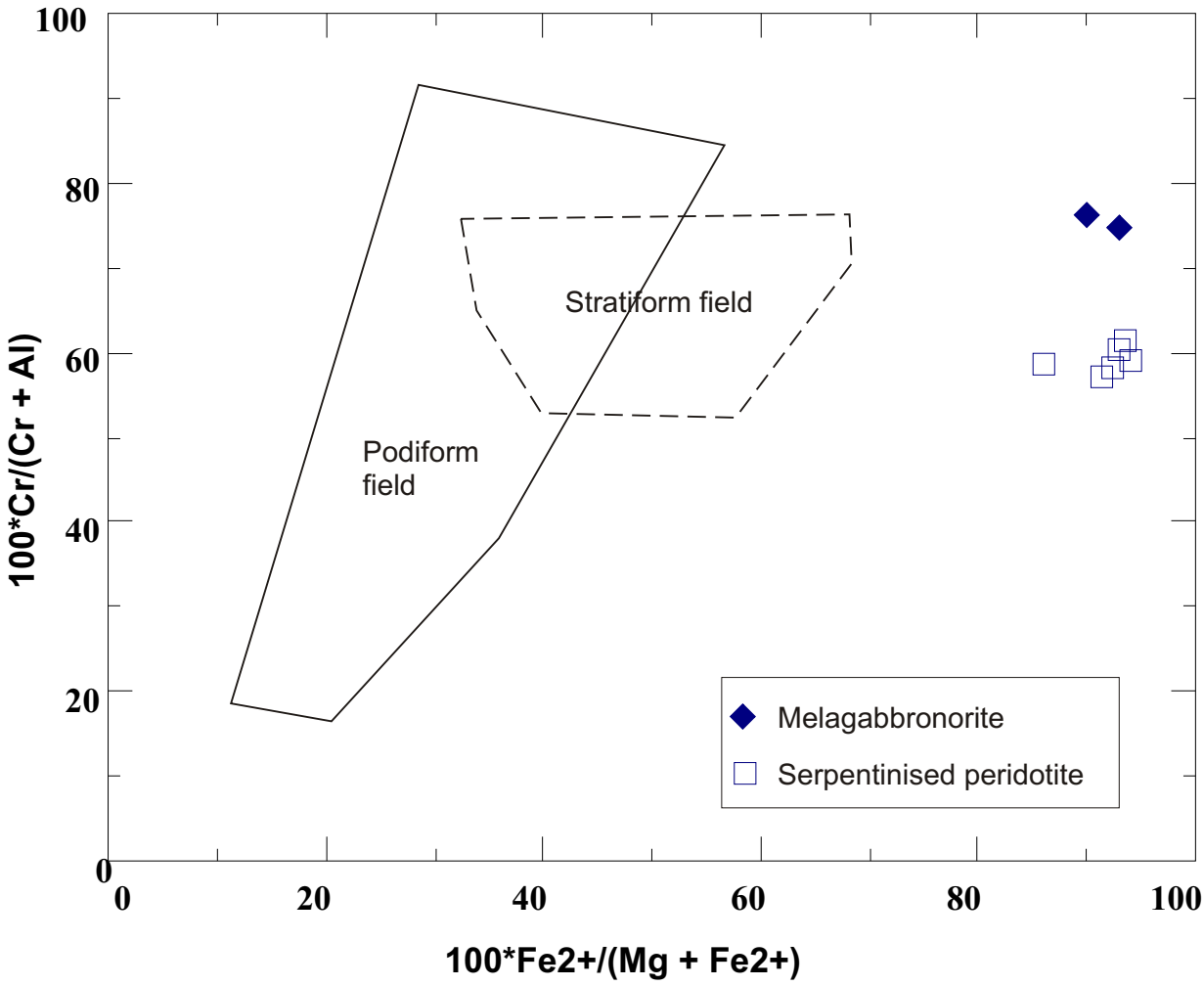

Fig. 8.7a: Cr # versus Fe # of the analysed Cr-bearing spinels from serpentinized peridotite (MO 26) and from melagabbronorites (MO 27).

compositions of Cr-bearing magnetites especially in serpentinised peridotites may be explained by subsolidus equilibration with ultramafic minerals (pyroxenes and olivines).

8.4 Summary and Discussion

The relative abundances of the sulphide minerals on Nonnenwerth are, in decreasing order, **pyrrhotite, chalcopyrite** and **pentlandite.** Textures, mineral assemblages and mineral chemistry point to a "typical magmatic" sulphide assemblage (e.g. Naldrett, 1989) that developed down-temperature from immiscible sulphide droplets in the silicate magma. Pyrite occurs locally and sphalerite, violarite and mackinawite occur in trace amounts.

In contrast, samples from Townlands are characterized by **chalcopyrite > millerite > pyrite > pentlandite**. Pyrrhotite occurs locally only and galena and molybdenite are further accessories. This sulphide assemblage differs from being "typical magmatic" and came into existence through syn- to post-magmatic modification at elevated fugacity of sulphur (fS_2).

The estimated abundance of sulphides, oxides and PGM in selected samples from Nonnenwerth and Townlands is given in Table 5 and some interrelationships are marked in colour.

Table 5: Estimated abundance of sulphides, oxides and PGM in polished thin sections from Nonnenwerth and Townlands

Sample	Sulphide abundance (%)	po	cpy	pn	py	mil	cr	mt	ilm	PGM	others
Nonnenwerth											
MOX9	1		+++	++	+++					Pd,Te Pt,Te Pt,Pd,Te	
MOX10	1	+++	++	++	+			+	+	Pt,Te Pt,Pd,S	
MOX11	2	+++	+++	+	+			+			
MOX12	2-3	+++	++	++				++	+	Pd,Te Au	
MOX14	< 1		+++	+/o	+++			++			
MOX15	1-2	+++	++	++							
MOX16	1	+++	+++	+				++	+		
MOX27	3-4	+++	+++	+++	++			++			
MOX29	20	+	+++	+	+			+		Pd,Te Pd,Pt,Bi,Te Pd,Bi,Te	hm
MOX30	10	+++	+	+	++			+			
MOX32	2	+++	+++	+	++		+		+		
MOX33	4-6	+++	+++	+				++			
Townlands											
P1	1	++	+++		+			+			
P2	5		++	+++		+		+++			viol
P4			++		++	++		++	+		hm
P7	30		++		+++	++		++		Pd,Fe,As	
P11	1-2	++	++		+++			+			
P12	5	+++	++	+++				+++			
P13		+++	++	++			++	++		Pd,Bi,Te Pd,Te,As Pt,As	moly
P14	20	+	++		+++	+++		++			ga, moly
P15	15-20	+/o	++		+++	+	+		+		
P19	20		++		+++	++		++			
P20	2-3	+	++	++	+++			++			
P26	2		+++	++	++	++		++			
P106			++		+++	++		+++		Pd,Bi,Te Pd,Te	

Estimated frequency: +++ very frequent, ++ frequent, + minor, o rare

Abbreviations: po = pyrrhotite, cpy = chalcopyrite, pn = pentlandite, py = pyrite, mil = millerite, cr = chromite, mt = magnetite, ilm = ilmenite, PGM = platinum-group mineral, hm = hematite, ga = galena, moly = molybdenite.

Nonnenwerth

The relative abundances of the sulphide minerals on Nonnenwerth are, in decreasing order, **pyrrhotite, chalcopyrite** and **pentlandite.** Textures, mineral assemblages and mineral chemistry (for example, elevated Pd contents in pentlandite) basically point to a "typical magmatic" sulphide assemblage (e.g. Naldrett, 1989) that developed down-temperature from immiscible sulphide droplets in the silicate magma. Pyrite occurs locally and sphalerite, violarite and mackinawite occur in trace amounts.

The current study distinguishes three different associations of sulphide at Nonnenwerth, i.e. (i) the "typical" magmatic sulphides, (ii) secondary sulphides replacing magmatic sulphides, and (iii) sulphides associated with secondary silicates.

(i) Magmatic sulphides are interstitial to plagioclase and orthopyroxene in essentially unaltered or slightly altered samples. They are represented by composite grains of pyrrhotite often intergrown with chalcopyrite and pentlandite, chalcopyrite and polycrystalline fragmented pentlandite grains along pyrrhotite fractures or pentlandite and chalcopyrite included in pyrrhotite towards pyrrhotite grain margins (Fig. 8.1a to e). Pentlandite may occur as flame-like exsolution lamellae in pyrrhotite. These magmatic sulphides represent fractionated blebs of sulphide. During crystallization, magmatic sulphide liquid crystallizes to a monosulphide solid solution (mss) with the residual sulphide liquid forming intermediate solid solution (iss) (Barnes *et al*., 2006). The former recrystallizes to pyrrhotite and pentlandite on cooling and the latter to chalcopyrite and some

pentlandite (Barnes *et al*., 2006) in agreement with the textures displayed by magmatic sulphides.

(ii) Secondary sulphides, as defined here, replace magmatic sulphides and lack the zoned, fractionated textures displayed by magmatic sulphides and have a 'rugged' outline. They are dominated by chalcopyrite, pyrite, and minor pentlandite. Pyrrhotite includes subrounded vermicular intergrowths of pyrite and chalcopyrite, in places with a remnant pentlandite suggesting replacement of pentlandite by the two phases (Fig. 8.3d, e and f). Pentlandite may be altered and replaced by coronas of violarite with relict pentlandite forming islands in violarite suggesting that the pentlandite is relictic and that most of the primary pentlandite has been replaced by violarite (Fig. 8.3h and i). It should be noted that recrystallized gabbronorite samples with high pyrrhotite contents have no pyrite and vice versa. The absence of pyrrhotite may suggest an increase in S fugacity (fS_2) resulting in pyrrhotite being transformed to or replaced by pyrite. Minor phases are fine, flame-like exsolutions of mackinawite and small disseminated sphalerite grains in chalcopyrite.

(iii) Sulphides associated with secondary silicate assemblages are rare in the Platreef at Nonnenwerth. They are represented by fine disseminated chalcopyrite grains intergrown with alteration minerals in replacement of primary silicates adjacent to coarse composite sulphides, deuteric veinlets of pyrite that cut through the plagioclase (Fig. 8.2i and j) or pyrite replacing clinopyroxene along cleavage planes and cracks (Fig. 8.3i). The sulphides do not display well defined sulphide zonation.

Townlands

In contrast to Nonnenwerth, samples from Townlands are characterized by **chalcopyrite > millerite > pyrite > pentlandite**. Pyrrhotite occurs locally only and galena and molybdenite are further accessories. Notably, this is the first time that such a sulphide assemblage is reported from the Platreef. This type of mineralization was detected in one drill hole only and therefore, must at this stage be regarded as exceptional and probably local only.

This sulphide assemblage differs from being "typical magmatic" and came into existence through syn- to post-magmatic modification including formation of millerite from pentlandite, and pyrite replacing pyrrhotite. It is envisaged that the sulphide assemblage at Townlands originally also developed from immiscible magmatic sulphide droplets and an association pyrrhotite – pentlandite – chalcopyrite. However, this early formation was overprinted and converted to pyrite – millerite – chalcopyrite. The observed sulphide assemblage gives evidence that the conversion took place at elevated fugacity of sulphur (fS_2) as will be shown below. This conversion was not completely pervasive, as evidenced by relict pyrrhotite – pentlandite assemblages (Table 5). Furthermore, no direct replacements (millerite after pentlandite and pyrite after pyrrhotite) were observed in situ.

The relative timing of this remobilization and replacement is hard to constrain; it probably took place early on the down-temperature path of the mineralization. Probably, syn- to post-emplacement fluids were also involved as evidenced by amphibole needles crosscutting sulphide grains (Fig. 8.4a).

An attempt is made to estimate the fO_2 and fS_2 in the Fe-Ni-S-O system under conditions of common hypogene equilibrium in altered ultramafic rocks (Eckstrand, 1975). The nature of the sulphide assemblage (pyrite, paucity of pyrrhotite, presence of millerite instead of pentlandite, presence of magnetite) suggest that its crystallisation occurred at elevated fugacities of sulphur and oxygen. The sulphides from the sulphide-poor rocks at the top of each Unit formed under moderate fS_2 and low fO_2 conditions (Eckstrand, 1975; Fig. 8.8). This is in agreement with the observed sulphide assemblages represented by assemblage 1 and 2 in Fig. 8.8b. In contrast, the sulphide-rich assemblage that occurs towards the base of each Unit probably formed under high fS_2 and fO_2 conditions (assemblage 3 in Fig. 8.8b). This model is thus in agreement with the observed sulphide assemblages and available S-isotope data (Manyeruke, 2003; Manyeruke *et al.*, 2005). Values of $d^{34}S$ increase towards the base of the Middle and Upper Platreef (Manyeruke, 2003), a phenomenon that was attributed to enhanced assimilation of crustal S towards the base of each layer, perhaps by continued degassing of the floor rocks during crystallisation of the Platreef. The high O fugacity may also be attributed to assimilation of dolomite followed by devolatization of the dolomite xenoliths and oxidation of the magma (de Waal, 1977).

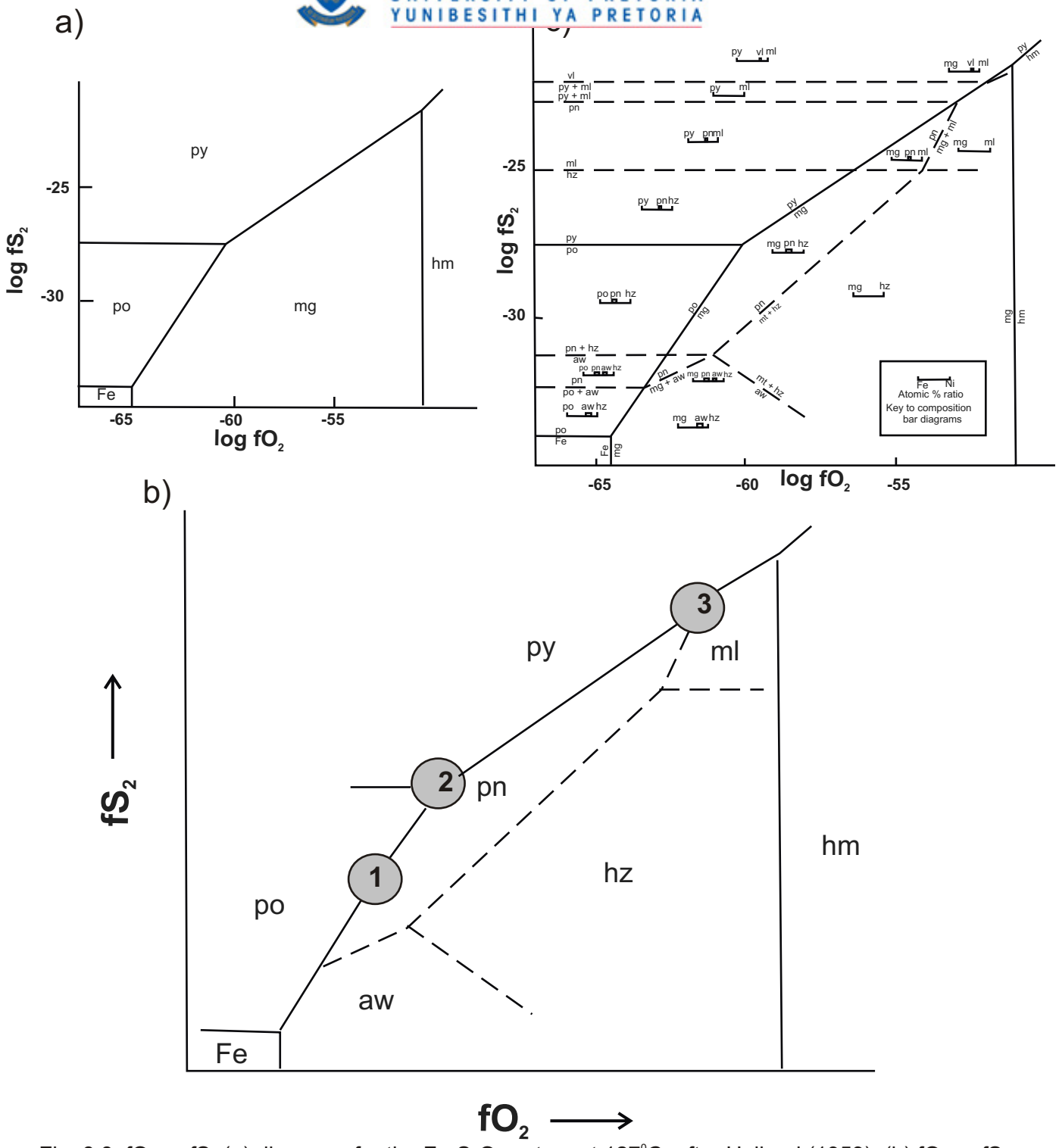

Fig. 8.8. fO_2 vs fS_2 (a) diagrams for the Fe-S-O system at 127^{0}C, after Holland (1959). (b) fO_2 vs fS_2 diagram for the Fe-Ni-S-O system at about 127^{0}C. Reaction boundaries for the Fe-S-O sub-system are shown as solid lines; others for which thermodynamic data are unavailable or unreliable are shown in dashed lines. (c) Approximate fO_2 vs fS_2 diagram for the Fe-Ni-S-O system under conditions of common hypogene equilibrium in altered ultramafic rocks, probably less than 200^{0}C. Assemblages noted in the Platreef on Townlands are shown by circled numbers on the appropriate field of the boundary. Assemblage 1 is composed of pyrrhotite, chalcopyrite, pentlandite ± magnetite, assemblage 2 is characterised by pyrite, pentlandite, chalcopyrite and minor pyrrhotite and assemblage 3 is characterized by pyrite, millerite, chalcopyrite ± pentlandite ± galena, molybdenite and magnetite. Figures modified after Eckstrand (1975).

As outlined above, the lack of a "typical "magmatic sulphide assemblage at Townlands may be the result of a number of possible processes. However, S-assimilation from the floor rocks shales is favoured here for the following reasons: Manyeruke (2003) and Manyeruke *et al.* (2005) have shown that $d^{34}S$ values in the Platreef at Townlands increase towards the base of the Middle and Upper Platreef, a phenomenon that was attributed to enhanced assimilation of crustal S towards the base of each layer, perhaps by continued degassing of the floor rocks during crystallisation of the Platreef. This is supported by the increase in the abundance of sulphides towards the base of each Unit at Townlands (Manyeruke, 2003: Manyeruke et al., 2005). The additional sedimentary sulphur probably reacted and totally modified the magmatic assemblage resulting in the paucity of "typical" magmatic sulphides at Townlands. This would suggest primary sulphide mineralization in the Platreef is of magmatic origin and contamination with floor rock sulphur. at Townlands (Manyeruke, 2003; Manyeruke *et al*., 2005) is a localised process in areas where the floor rocks are sulphur- bearing.

PGE

With the exception of pentlandite from Nonnenwerth (see below), Pd, Pt and Rh are below the detection limits of the electron microprobe in the sulphides analysed from Nonnenwerth and Townlands.

Pentlandites as part of the "typical magmatic" sulphide assemblage at Nonnenwerth constantly contain appreciable amounts of Pd (range from ~ 140 – 700 ppm). This finding is in accordance with literature data (e.g. Gervilla et al., 2004) that pentlandite may carry even up to some % of Pd (substituting for Ni) in

its crystal lattice. Accordingly, the Pd contents in Nonnenwerth pentlandite probably reflect a primary magmatic signature.

In contrast, pentlandites from Townlands have Pd contents below the detection limit (20 ppm Pd) of the method. This lack of measurable Pd contents in pentlandite may find the following explanations:

(i) Pd in pentlandite was analysed in one sample (P 13) only, and therefore, the results may not be representative.

(ii) Pd-bearing PGM could have been mobilized during replacement of 'primary' sulphides by pyrite dominated assemblages into the surrounding silicates (Prichard *et al*., 2001).

(iii) The Townlands sulphide assemblage differs from being "typical magmatic" and has experienced severe syn- to post-magmatic modification as described above. Therefore, the relatively rare pentlandite at Townlands may either represent a second generation of pentlandite, or is a relict primary phase that has suffered an overprint that extracted lattice-bound Pd. Arguments for the latter possibility are provided by the presence of abundant Pd-minerals in sample P 13 (see Table 5).

The analytical work presented here has shown marked differences in Pd contents in pentlandites from the Platreef for the first time. It is suggested that systematic research in this topic would be a worthwhile undertaking to improve our understanding of the distribution of the PGE in Platreef ores.

The nature and distribution of the PGM from Nonnenwerth and Townlands are documented in the next chapter (Chapter 9).